Electronic Supporting Information

CuO stabilized on magnetic decorated GO nanosheets efficiently promoted the one-pot synthesis of 3,4-dihydropyrimidine-2(1*H*)-one/thione and 1,4-dihydropyridine derivatives under green chemistry conditions

Mohammad Eslami,[a,b] Mohammad G. Dekamin,*[b] Elham Mahdavi[b]

[a]*Department of Chemistry, Behbahan Khatam Alanbia University of Technology, Behbahan 63616-63973, Iran.*

[b]*Pharmaceutical and Heterocyclic Compounds Research Laboratory, Department of Chemistry, Iran University of Science and Technology, Tehran, 1684613114, Iran.* Email: mdekamin@iust.ac.ir

CONTENTS

Experimental

Materials

All starting materials, reagents and solvents are commercially available and were purchased from Merck or Aldrich and used without further purification, except for benzaldehyde which was used as a fresh distilled sample. ^{1}H NMR spectra were recorded on a Bruker (Avance DRX-500) spectrometer using $CDCl_3$ as solvent at room temperature. Chemical shifts δ are reported in parts per million (ppm) relative to tetramethylsilane as an internal standard. Fourier Transform infrared (FT-IR) spectra of samples were measured using an ABB Bomem MB100 FTIR spectrophotometer. CHNS analysis was done by LECO Truspec. Scanning electron microscopy (SEM) was performed on VEGA\\TESCAN-LMU. An energy dispersive detector (EDS) coupled to the microscope was used to identify chemical elements of the prepared catalyst. X-ray diffraction (XRD) pattern was recorded on APD 2000, using Cu Kα radiation (50 kV, 150 mA) in the range 2θ =10-120°.

Synthesis of Graphene Oxide (GO):

The graphene oxide (GO) sheets were prepared by a modified Hummers´ method according to the method reported in the literature.108

Synthesis of Benzotriazole (BTA):

5.4 g of *o*-phenylenediamine was dissolved in a mixture containing 6.0 mL of glacial acetic acid and 20 mL of water. The solution was subsequently cooled to 15°C. A separate solution of 3.0 g of sodium nitrite dissolved in 7 mL of water was then gradually introduced into the reaction mixture. Upon addition, a noticeable color change from deep red to pale brown was observed. The reaction mixture was further cooled in an ice bath for 30 minutes. The resulting benzotriazole product was isolated through filtration and subsequently washed with cold water to ensure purity.

Synthesis of 1-(prop-2-yn-1-yl)-1H-benzo[d][1,2,3]triazole:

In the subsequent step, 2.0 mmol of the synthesized benzotriazole, 2.2 mmol of propargyl bromide, 4.0 mmol of potassium carbonate, and 5 mL of DMF were introduced into a reaction flask. The mixture was stirred at 45°C for 12 hours. Reaction progress was monitored via thin-layer chromatography using a solvent system of ethyl acetate (1:3). Upon completion, the product, 1-(prop-2-yn-1-yl)-1*H*-benzo[*d*][1,2,3]triazole, was isolated through extraction with ethyl acetoacetate and subsequently dried in an oven to obtain the final compound.

Synthesis of 1-((1*H*-1,2,3-triazol-5-yl)methyl)-1*H*-benzo[*d*][1,2,3]triazole:

The grafting of 1-(prop-2-yn-1-yl)-1*H*-benzo[*d*][1,2,3]triazole onto magnetic graphene oxide was carried out via a click reaction. Initially, 300.0 mg of graphene oxide was dispersed in 80 mL of deionized water through ultrasonication. To this dispersion, 10.0 mmol of 1-(prop-2-yn-1-yl)-1*H*-benzo[*d*][1,2,3]triazole, 15.0 mmol of sodium azide, 20 mol% of sodium ascorbate, 0.5 mmol of copper sulfate, and 20 mL of tert-butyl alcohol were added. The reaction mixture was stirred at 60°C for 24 hours. Upon completion, the nanocomposite was isolated using an external magnetic field and thoroughly washed with distilled water (3*10 mL) and ethanol (1*10 mL), then dried at 50°C.

Synthesis of CuO/mGO-TA-Me-BTA nano-catalyst:

In a 250 mL reaction vessel, 1.0 g of magnetic graphene oxide nanocomposite grafted with benzotriazole (CuO/mGO-TA-Me-BTA) was dispersed in 100 mL of deionized water through ultrasonication. To this dispersion, 3.0 mmol of copper(II) sulfate dissolved in 25 mL of deionized water was added, and the mixture was stirred at room temperature for 24 hours.

Afterward, the nanocomposite was isolated using an external magnetic field, washed with distilled water, and dried under vacuum. The structure of the synthesized nanocomposite (CuO/mGO-TA-Me-BTA) was characterized by FT-IR, XRD, SEM, EDX, elemental mapping, TGA, VSM, and AAS analyses.

One-pot, three-component synthesis of 3,4-dihydropyrimidin-2-one/thion derivatives in the presence of CuO/mGO-TA-Me-BTA magnetic nanoparticles (4a-w):

For the synthesis of 3,4-dihydropyrimidinone derivatives, a mixture of 1.0 mmol aldehyde, 1.1 mmol urea (or thiourea), 1.0 mmol ethyl acetoacetate, and 10.0 mg of the CuO/mGO-TA-Me-BTA nanocomposite as a catalyst was added to a 5 mL round-bottom flask along with 1.5 mL distilled water and 0.5 mL ethanol. The reaction mixture was stirred using a magnetic stirrer and heated under reflux in an oil bath for the required time, as indicated in **Table 2**. The progress of the reaction was monitored by thin-layer chromatography (TLC) using a solvent system of 1:3 n-hexane:acetate. Upon completion of the reaction, the magnetic nanocatalyst was separated using an external magnetic field, and the 3,4-dihydropyrimidinone product was isolated by extraction with ethyl acetate. If necessary, the products were crystallized from a mixture of ethyl acetate-n-hexane or ethanol. The final structures of the synthesized compounds were identified and confirmed by M.P (Melting Point), ^{1}H NMR, and FT-IR analyses.

One-pot, three-component synthesis of 1,4-Dihydropyridine derivatives in the presence of CuO/mGO-TA-Me-BTA magnetic nanoparticles (6a-m):

For the synthesis of 1,4-dihydropyridine derivatives, a 5 mL round-bottom flask was filled with a mixture of 1.0 mmol aldehyde, 2.0 mmol ethyl acetoacetate, 1.5 mmol ammonium acetate, 10 mg of CuO/mGO-TA-Me-BTA nanocomposite as the catalyst, 1.5 mL distilled water, and 0.5 mL ethanol as the solvent. The reaction mixture was stirred with a magnetic stirrer and heated under reflux in an oil bath for the duration specified in **Table 3**. Reaction progress was monitored by thin-layer chromatography (TLC) using a 1:3 n-hexane:ethylacetate solvent system. After the reaction was complete, the magnetic nanocatalyst was separated using an external magnetic field, and the 1,4-dihydropyridine product was extracted with ethyl acetate. If needed, the products were crystallized from a mixture of ethyl acetate and n-hexane or ethanol. The final structures of the synthesized compounds were confirmed by melting point (M.P) determination, ^{1}H NMR, and FT-IR spectroscopy.

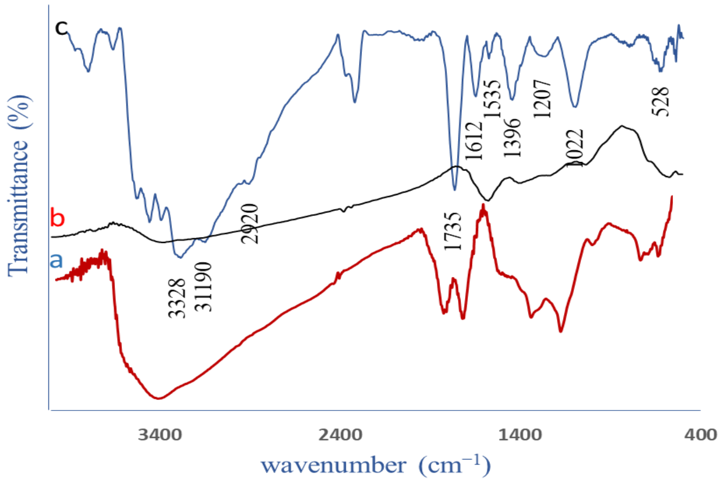

Fig. S1. FTIR spectra of **a)** GO, **b)** mGO, and **c)** the CuO/mGO-TA-Me-BTA.

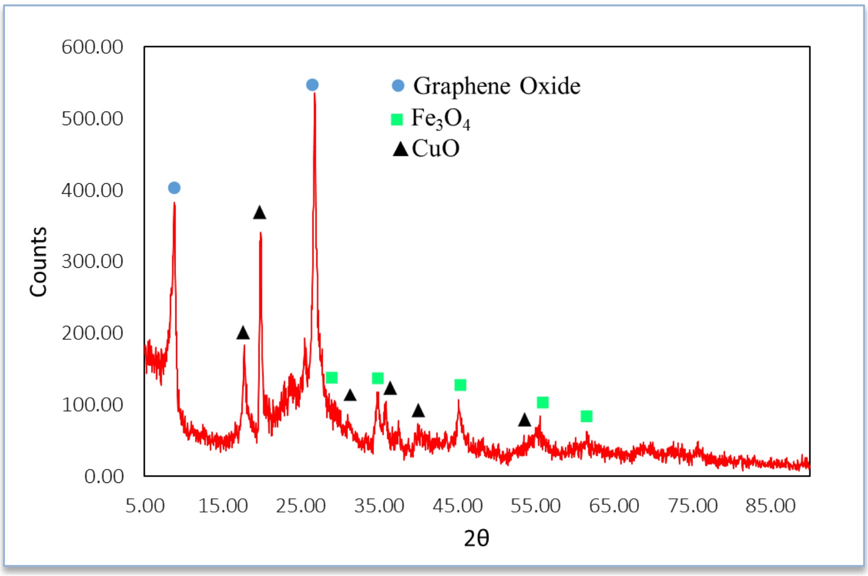

Fig. S2. XRD pattern of the CuO/mGO-TA-Me-BTA nanocatalyst.

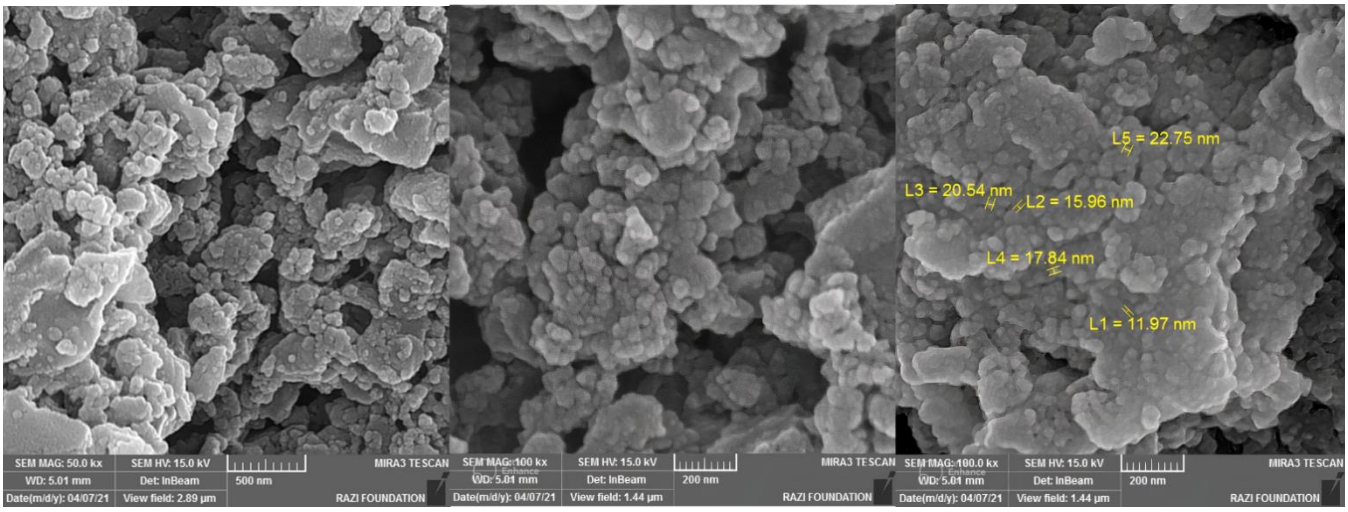

Fig. S3. FESEM images of the CuO/mGO-TA-Me-BTA nanocatalyst.

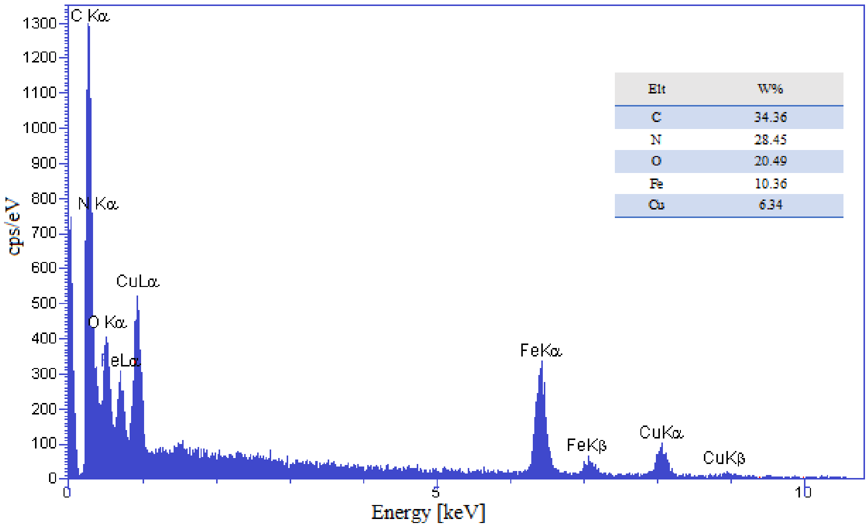

Elt	W%
C	34.36
N	28.45
O	20.49
Fe	10.36
Cu	6.34

Fig. S4. EDX pattern of the CuO/mGO-TA-Me-BTA nanocatalyst.

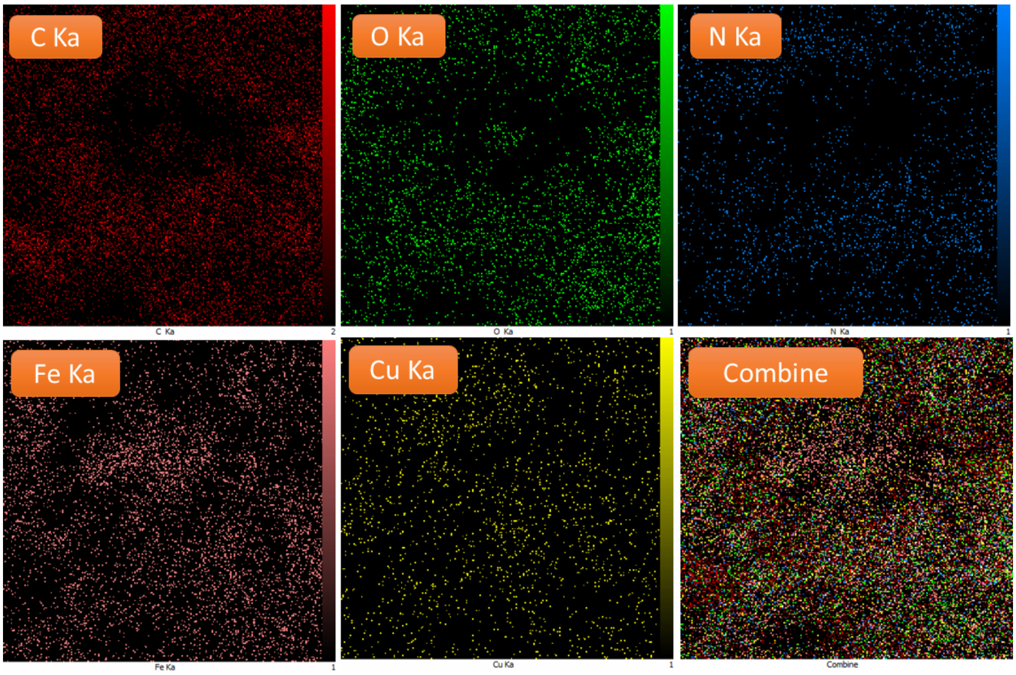

Fig. S5. Elemental mapping of different elementals in the structure of CuO/mGO-TA-Me-BTA nanocatalyst.

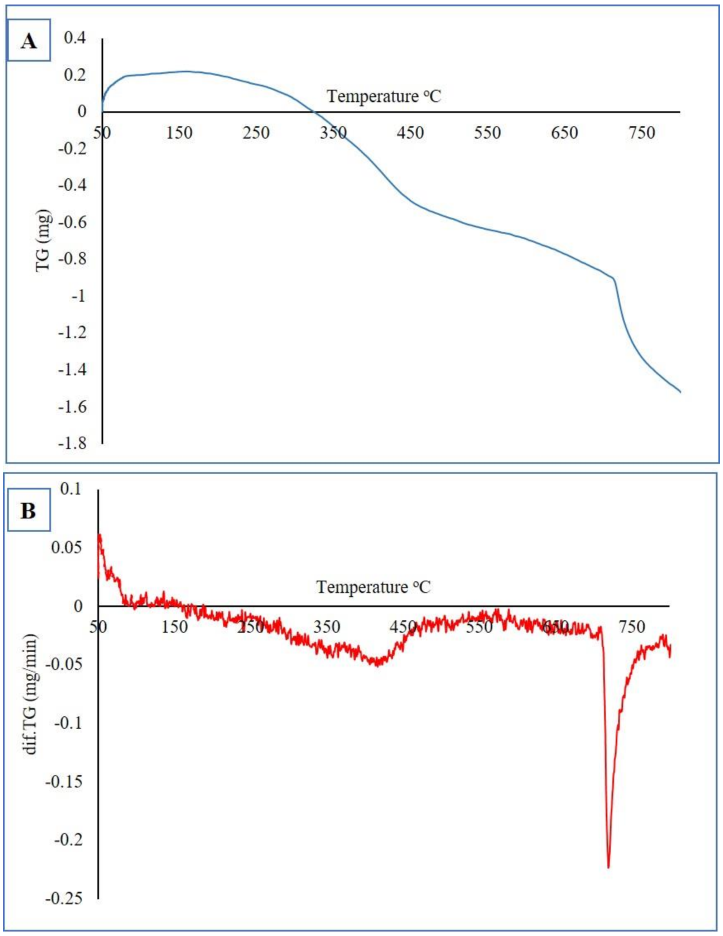

Fig. S6. a) TGA, **b**) DTA curves for the CuO/mGO-TA-Me-BTA nanocatalyst.

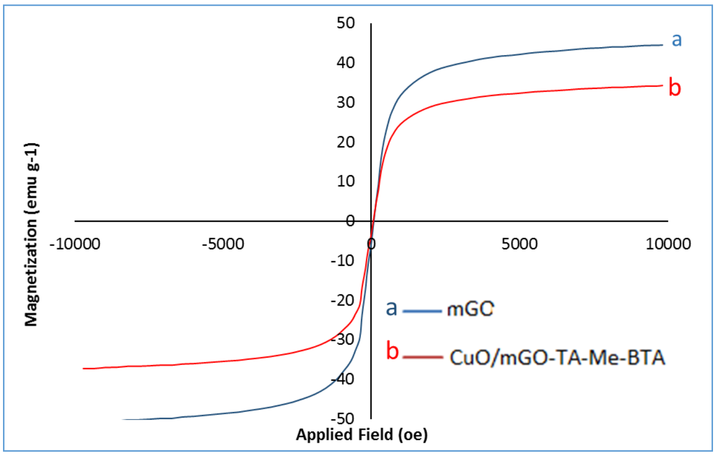

Fig. S7. Magnetization curves for **a**) mGO nano sheets and **b**) CuO/mGO-TA-Me-BTA nanocatalyst.

Spectroscopic characterization of the products 4e, 4m, 4n, 4t, 4u, 6c, 6h, and 6l.

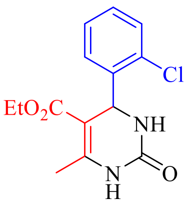

Ethy l-4-(2-chlorophenyl)-6-methyl-2-oxo-1,2,3,4-tetrahydropyrimidine-5-carboxylate (4**e**, entry 5, Table 2); White solid; M.P: 206-207 °C, ^{1}H NMR (500 MHz, DMSO-d_6, δ = ppm) δ: 9.3 (s, 1H, NH), 7.68 (s, 1H, NH), 7.39 (d, 1H, *J* = 7.5 Hz, ArH), 7.26-7.30 (m, 3H, ArH), 5.6 (s, 1H, CH), 3.89 (q, *J* = 7.1 Hz, 2H, CH_2), 2.29 (s, 3H, CH_3), 0.98 (t, *J* = 6.5, 3H, CH_3); FT-IR (KBr, disk) ν (cm^{-1}): 3354 (NH stretch for amide), 3229(NH stretch for amide), 3111 (Ar-H stretch), 2972 (CH_2CH_3, CH_3 stretch), 2869 (CH_2 stretch), 1695 (C=C-CO-OR, C=O stretch), 1642 (RCONHR`, C=O stretch), 1593 (C=C stretch), 1445 (Ar C-C stretch), 1370 ($RCH_2CH_3$, $CH_2$), 1322 ($CH_3$), 1225 (RCOOR`, C-O stretch), 1092 (RCONHR`, C-O stretch), 1027 (C-N stretch),745 (C-Cl stretch).

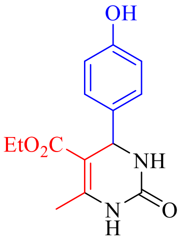

Ethyl 4-(4-hydroxyphenyl)-6-methyl-2-oxo-1,2,3,4-tetrahydropyrimidine-5-carboxylate (**4m**, entry 13, Table 2); White solid; M.P: 232-233 °C, ^{1}H NMR (500 MHz, DMSO-d_6, δ = ppm) δ: 12.89 (1H, br, OH), 9.25 (s, 1H, NH), 7.90 (d, 2H, *J* = 8.0 Hz, ArH), 7.80 (s, br, 1H, NH), 7.34 (d, 2H, *J* = 8.0 Hz, ArH), 5.20 (s, 1H, CH), 3.98 (q, *J* = 7.0 Hz, 2H, CH_2), 2.25 (s, 3H, CH_3), 1.08 (t, *J* = 7.0, 3H, CH_3); FT-IR (KBr, disk) ν (cm^{-1}): 3510 (OH stretch), 3359 (NH stretch for amide), 3232 (NH stretch for amide), 3122 (Ar-H stretch), 2997 (CH_2CH_3, CH_3 stretch), 2821 (CH_2 stretch), 1689 (C=C-CO-OR, C=O stretch), 1643 (RCONHR`, C=O stretch), 1481 (C=C stretch), 1460 (Ar C-C stretch), 1377 ($RCH_2CH_3$, $CH_2$), 1300 ($CH_3$), 1238 (RCOOR`, C-O stretch), 1087 (RCONHR`, C-O stretch), 1008 (C-N stretch).

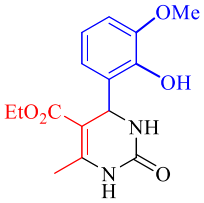

Ethyl 4-(2-hydroxy-3-methoxyphenyl)-6-methyl-2-oxo-1,2,3,4-tetrahydropyrimidine-5-carboxylate (**4n**, entry 14, Table 2); White solid; M.P: 238 °C, ^{1}H NMR (500 MHz, DMSO-d_6, δ = ppm) δ: 9.08 (s, 1H, NH), 8.73 (s, 1H, OH), 7.06 (1H, br, OH), 6.74 (d, 1H, *J* = 7.0 Hz, ArH), 6.69 (t, 1H, *J* = 8.0 Hz, ArH), 6.61 (d, 1H, *J* = 7.5 Hz, ArH), 5.54 (d, *J* = 2.5 Hz, 1H, CH), 3.92 (d of q, *J* = 9.0 Hz, 2H, CH_2), 3.77 (s, 3H, OCH_3), 2.96 (s, 3H, CH_3), 1.03 (t, *J* = 7.0, 3H, CH_3); FT-IR (KBr, disk) ν (cm^{-1}): 3507 (OH stretch for amide), 3353 (NH stretch for amide), 3225 (NH stretch for amide), 3117 (Ar-H stretch), 2960 (CH_2CH_3, CH_3 stretch), 2840 (CH_2 stretch), 1686 (C=C-CO-OR, C=O stretch), 1640 (RCONHR`, C=O stretch), 1594 (C=C stretch), 1490 (Ar C-C stretch), 1370 ($RCH_2CH_3$, $CH_2$), 1340 ($CH_3$), 1281 (RCOOR`, C-O stretch), 1224 (Ar-O-R, C-O stretch), 1071 (RCONHR`, C-O stretch), 1025 (C-N stretch).

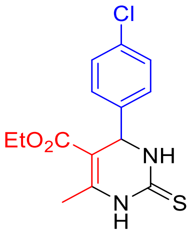

Ethyl 4-(4-chlorophenyl)-6-methyl-2-thioxo-1,2,3,4-tetrahydropyrimidine-5-carboxylate (**4t**, entry 20, Table 2); White solid; M.P: 188-190 °C, ^{1}H NMR (500 MHz, DMSO-d_6, δ = ppm) δ: 10.33 (s, 1H, NH), 9.62 (s, br, 1H, NH), 7.36 (d, 2H, *J* = 8.0 Hz, ArH), 7.16 (d, 1H, *J* = 8.0 Hz, ArH), 5.09 (s, 1H, CH), 3.94 (q, *J* = 7.0 Hz, 2H, CH_2), 2.23 (s, 3H, CH_3), 1.03 (t, *J* = 7.0, 3H, CH_3); FT-IR (KBr, disk) ν (cm^{-1}): 3325 (NH stretch for thioamide), 3172 (NH stretch for thioamide), 3097 (Ar-H stretch), 2997 (CH_2CH_3, CH_3 stretch), 2893 (CH_2 stretch), 1670 (C=C-CO-OR, C=O stretch), 1573 (RCSNHR`, C=S stretch), 1463 (Ar C-C stretch), 1381 ($RCH_2CH_3$, $CH_2$), 1328 ($CH_3$), 1284 (RCOOR`, C-O stretch), 1195 (C-S stretch), 1116 (RCONHR`, C-O stretch), 1014 (C-N stretch), 752 (C-Cl stretch).

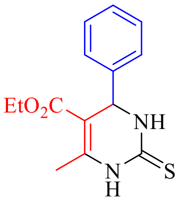

Ethyl 6-methyl-4-phenyl-2-thioxo-1,2,3,4-tetrahydropyrimidine-5-carboxylate (**4u**, entry 21, Table 2); White solid; M.P: 207-208 °C, ^{1}H NMR (500 MHz, DMSO-d_6, δ = ppm) δ: 10.29 (s, 1H, NH), 9.60 (s, br, 1H, NH), 7.28 (t, 2H, *J* = 7.0 Hz, ArH), 7.21 (t, 1H, *J* = 7.0 Hz, ArH), 7.15 (d, 2H, *J* = 7.0 Hz, ArH), 5.11 (d, *J* = 3.5 Hz, 1H, CH), 3.95 (q, *J* = 6.5 Hz, 2H, CH_2), 2.23 (s, 3H, CH_3), 1.04 (t, *J* = 7.0, 3H, CH_3); FT-IR (KBr, disk) ν (cm^{-1}): 3327 (NH stretch for thioamide), 3170 (NH stretch for thioamide), 3101 (Ar-H stretch), 2981 (CH_2CH_3, CH_3 stretch), 2895 (CH_2 stretch), 1670 (C=C-CO-OR, C=O stretch), 1573 (RCSNHR`, C=S stretch), 1462 (Ar C-C stretch), 1375 ($RCH_2CH_3$, $CH_2$), 1328 ($CH_3$), 1282 (RCOOR`, C-O stretch), 1197 (C-S stretch), 1114 (RCONHR`, C-O stretch), 1026 (C-N stretch).

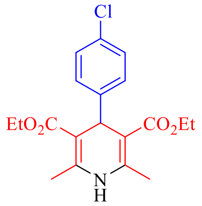

Diethy l2,6-dimethyl-4-(4-colorophenyl)-1,4-dihydropyridine-3,5-dicarboxylate (**6c** , entry 3, Table 3); White solid, M.P: 142 °C , ^{1}H NMR (500 MHz, $CDCl_3$, δ = ppm) δ: 7.20 (d, *J* = 8.5 Hz, 2H, Ar-H), 7.14 (d, *J* = 8.4 Hz, 2H, Ar-H), 5.74 (s, 1H, NH), 4.8 (s, 1H, CH), 4.1 (m, 4H, CH_2), 2.28 (s, 6H, CH_3), 1.2 (t , *J* = 7.1 Hz, 6H, CH_3); FT-IR (KBr, disk) ν (cm^{-1}) : 3361 (NH stretch for amine), 3096 (Ar-H stretch), 2989 (RCH_2CH_3, CH_3 stretch), 2928 (CH_2 stretch), 1697 (C=C-CO-OR, C=O stretch), 1654 (C=C-CO-OR, C=O stretch), 1636 (C=C stretch), 1489 (Ar C-C stretch), 1372 (RCH_2CH_3, CH_2 and CH_3), 1334 (CH_3), 1215 (RCOOR`, C-O stretch), 1119 (RCOOR`, C-O stretch), 1082 (C-N stretch), 785 (C-Cl stretch).

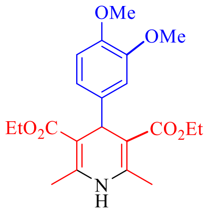

Diethyl 4-(3,4-dimethoxyphenyl)-2,6-dimethyl-1,4-dihydropyridine3,5-dicarboxylate (**6h**, entry 8, Table 3); White solid, M.P: 147-148 °C , ^{1}H NMR (500 MHz, $CDCl_3$, δ = ppm) δ: 6.87 (d, *J* = 2 Hz, 1H, ArH), 6.78 (dd, *J* = 2 Hz, 1H, ArH), 6.70 (d, *J* = 8.2 Hz, Ar-H), 5.95 (s, 1H, NH), 4.92 (s, 1H, CH), 4.08 (m, 4H, CH_2), 3.81 (s, 6H, CH_3O), 3.79 (s, 6H, CH_3O), 2.30 (s, 6H, CH_3),1.22 (t, *J* = 7.1 Hz, 6H, CH_3); FT-IR (KBr, disk) ν (cm^{-1}): 3345 (NH stretch for amine), 3094 (Ar-H stretch), 2983 (RCH_2CH_3, CH_3 stretch), 2928 (CH_2 stretch), 1688 (C=C-CO-OR, C=O stretch), 1653(C=C-CO-OR, C=O stretch), 1619 (C=C stretch), 1485 (Ar C-C stretch), 1368 (RCH_2CH_3, CH_2 and CH_3), 1322 (CH_3), 1257 (Ar-O-R, C-O stretch), 1227 (Ar-O-R, C-O), 1209 (RCOOR`, C-O stretch), 1138 (RCOOR`, C-O stretch), 1028 (C-N stretch).

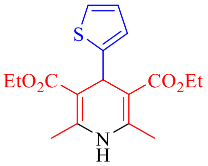

Diethyl2,6-dimethyl-4-(thiophen-2-yl)-1,4-dihydropyridine-3,5-dicarboxylate (**6l** , entry 12, Table 3); White solid, M.P: 170-171 °C , ^{1}H NMR (500 MHz, CDCl3 , δ = ppm) δ: 5.8 (s, 1H, NH) , 7.20 (t, *J*= 1.0 Hz, 1H, Het-Ar-H), 6.20 (dd, *J* = 2 Hz, 2H, Het-Ar-H), 5.94 (d, *J* = 3.0 Hz, 1H, Het-Ar-H), 5.82 (s, br, 1H, NH), 5.19 (s, 1H, CH), 4.15 (m, 4H, CH_2), 2.32 (s, 6H, CH_3), 1.24 (t, *J* = 7.31 Hz, 6H, CH_3); FT-IR (KBr, disk) ν(cm^{-1}): 3348 (NH stretch for amine), 3098 (Het-Ar-H stretch), 2985 (RCH_2CH_3, CH_3 stretch), 2903 (CH_2 stretch, CH_2 and CH_3), 1335 (CH_3), 1209 (RCOOR`, C-O stretch), 1121 (RCOOR`, C-O stretch), 1091 (C-N stretch), 807 (C-S stretch).

^{1}H NMR and FTIR spectra of the products 4e, 4m, 4n, 4t, 4u, 6c, 6h, and 6l

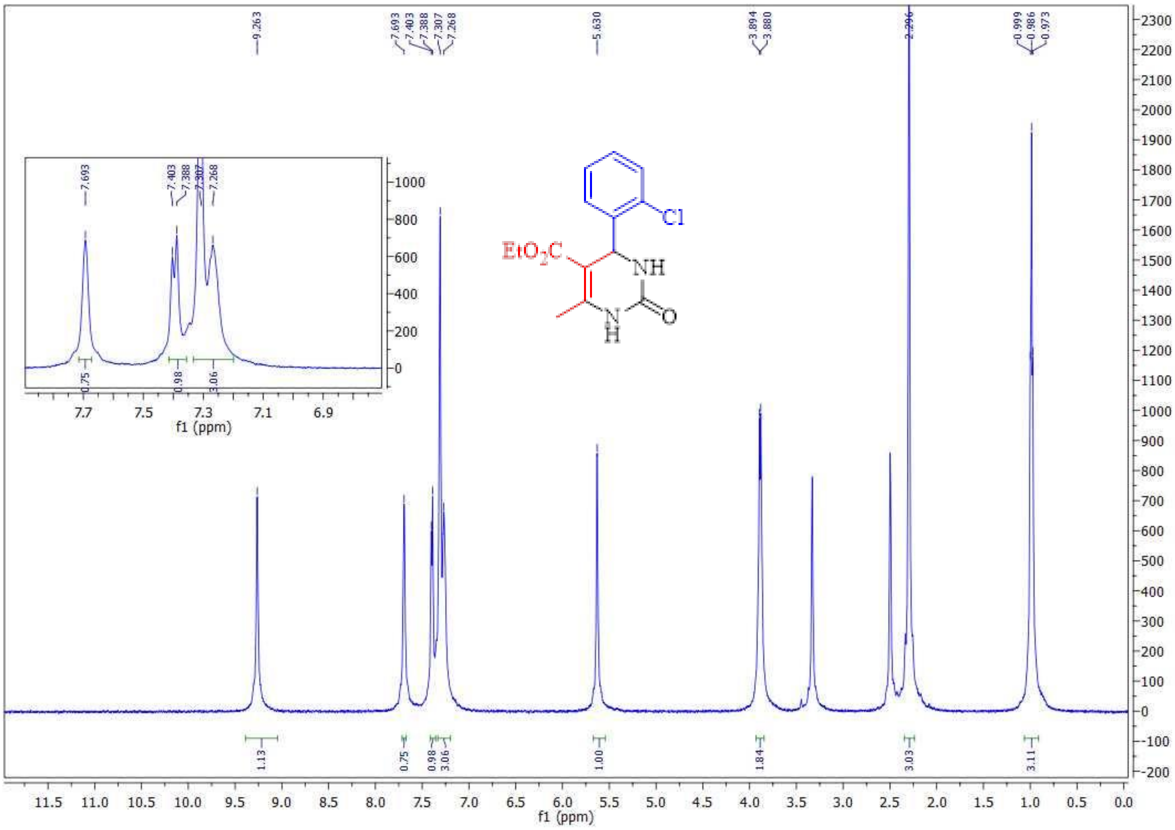

Fig. S8. ^{1}HNMR (500 MHz, DMSO-d_6) spectrum of Ethy l-4-(2-chlorophenyl)- 6-methyl-2-oxo-1,2,3,4-tetrahydropyrimidine-5-carboxylate (**4e**).

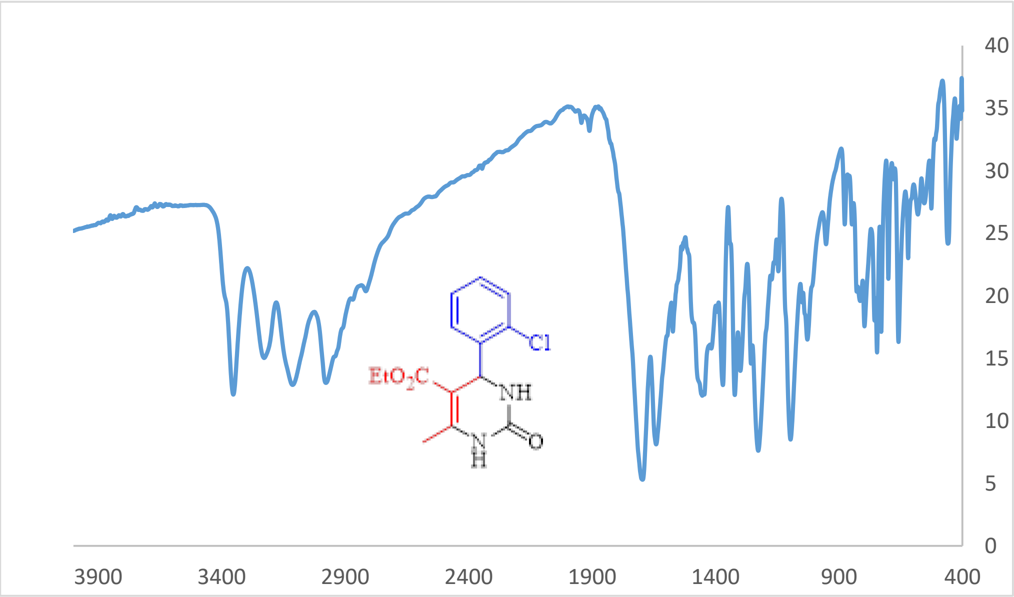

Fig. S9. FTIR spectrum of Ethy l-4-(2-chlorophenyl)-6-methyl-2-oxo-1,2,3,4-tetrahydropyrimidine-5-carboxylate (**4e**).

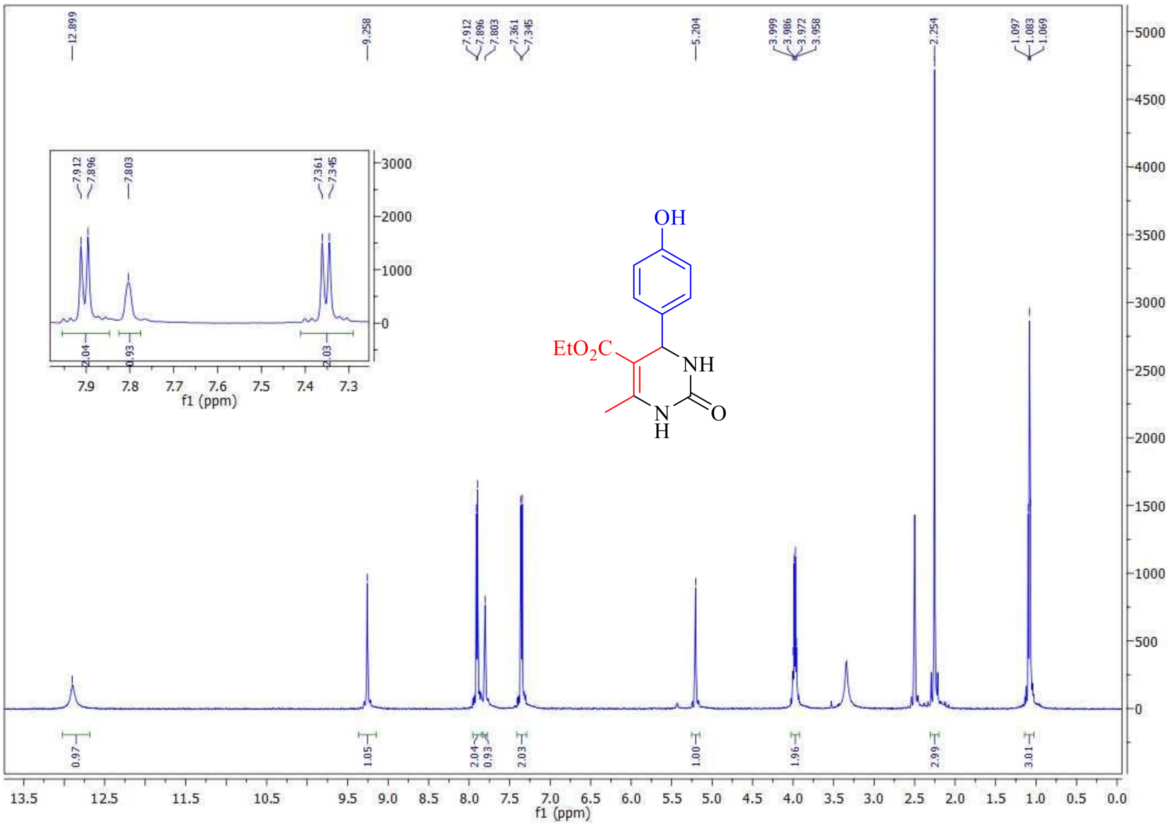

Fig. S10. ^{1}HNMR (500 MHz, DMSO-d$_6$) spectrum of Ethyl 4-(4-hydroxyphenyl)-6-methyl-2-oxo-1,2,3,4-tetrahydropyrimidine-5-carboxylate (**4m**).

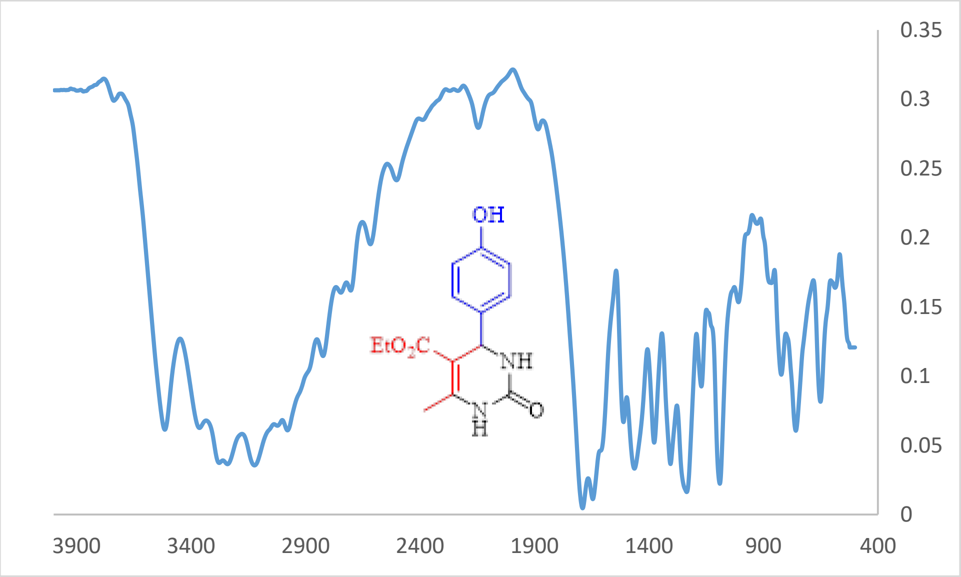

Fig. S11. FTIR spectrum of Ethyl 4-(4-hydroxyphenyl)-6-methyl-2-oxo-1,2,3,4-tetrahydropyrimidine-5-carboxylate (**4m**).

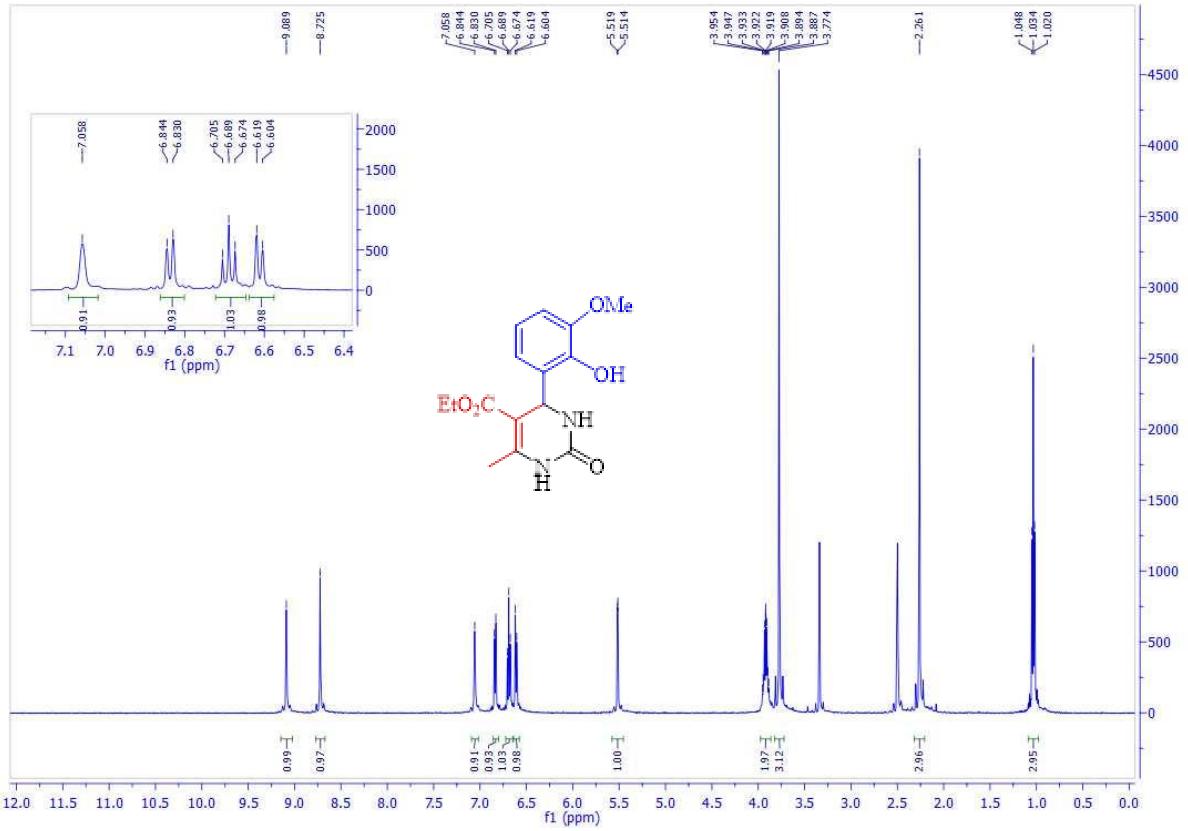

Fig. S12. ^{1}HNMR (500 MHz, DMSO-d$_6$) spectrum of Ethyl 4-(2-hydroxy-3-methoxyphenyl)-6-methyl-2-oxo-1,2,3,4-tetrahydropyrimidine-5-carboxylate (**4n**).

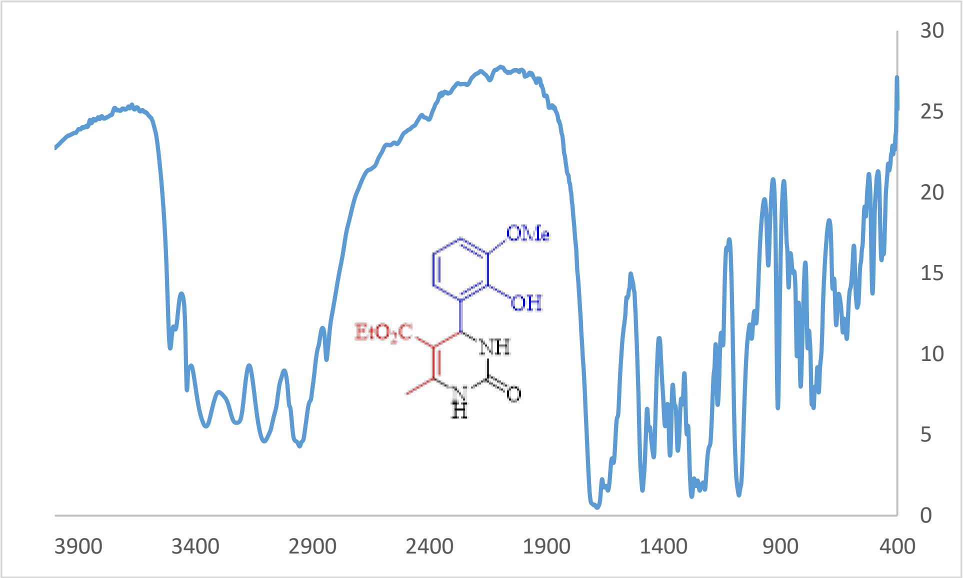

Fig. S13. FTIR spectrum of Ethyl 4-(2-hydroxy-3-methoxyphenyl)-6-methyl-2-oxo-1,2,3,4-tetrahydropyrimidine-5-carboxylate (**4n**).

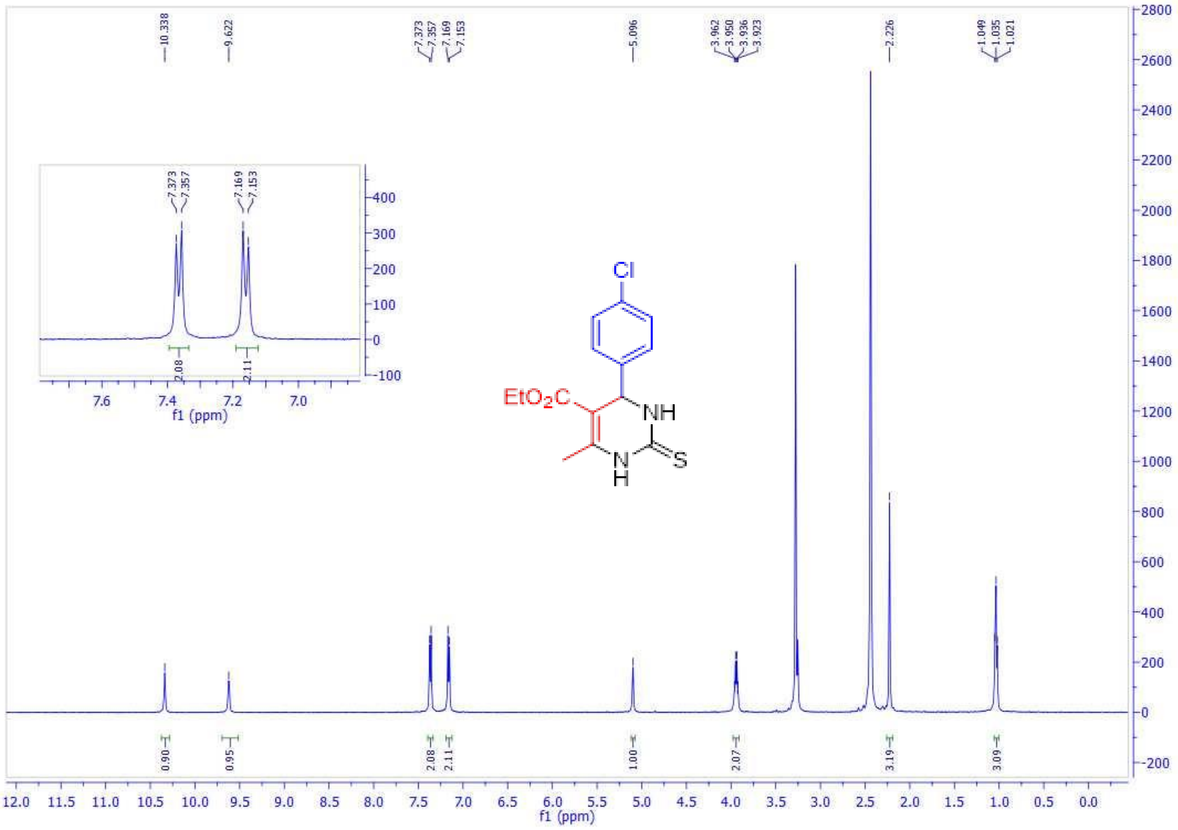

Fig. S14. ^{1}HNMR (500 MHz, DMSO-d_6) spectrum of Ethyl 4-(4-chlorophenyl)-6-methyl-2-thioxo-1,2,3,4-tetrahydropyrimidine-5-carboxylate (**4t**).

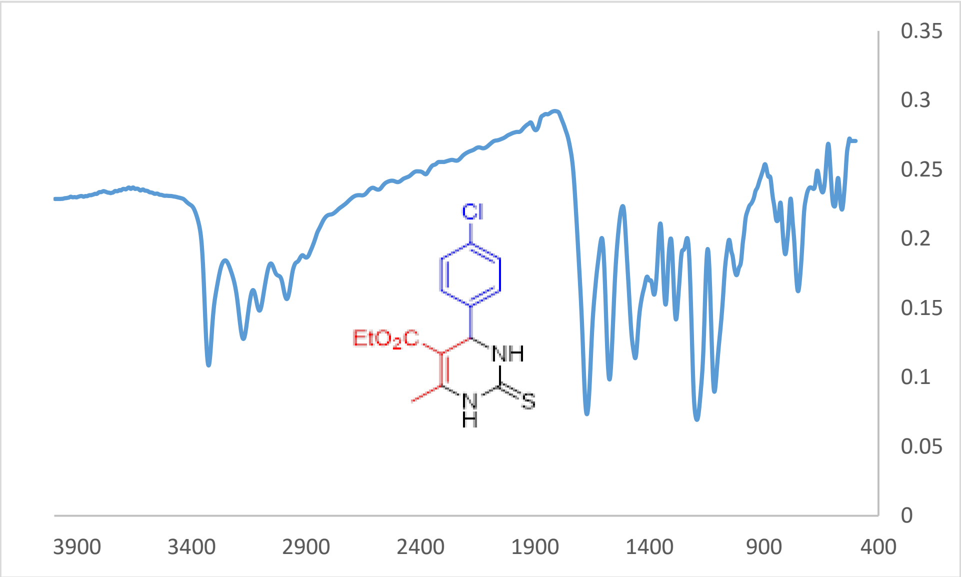

Fig. S15. FTIR spectrum of Ethyl 4-(4-chlorophenyl)-6-methyl-2-thioxo-1,2,3,4-tetrahydropyrimidine-5-carboxylate (**4t**).

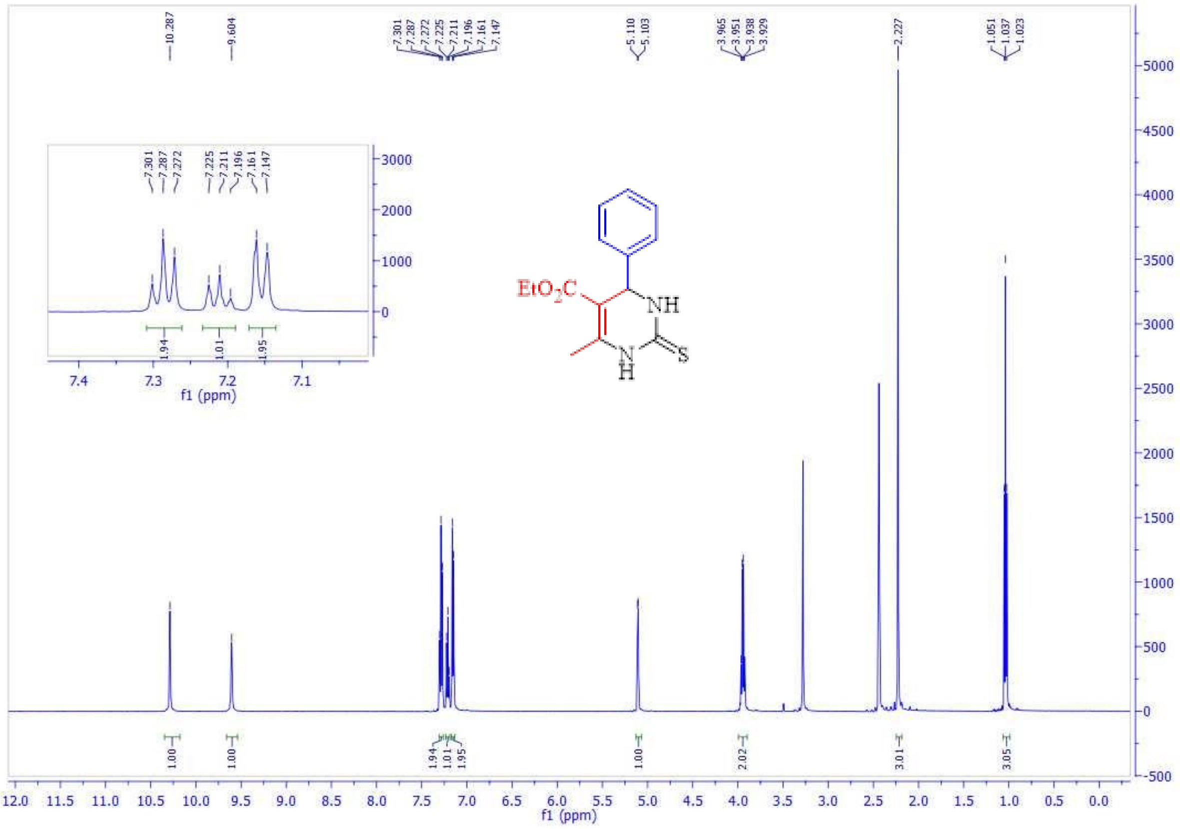

Fig. S16. ^{1}HNMR (500 MHz, DMSO-d$_6$) spectrum of Ethyl 6-methyl-4-phenyl-2-thioxo-1,2,3,4-tetrahydropyrimidine-5-carboxylate (**4u**).

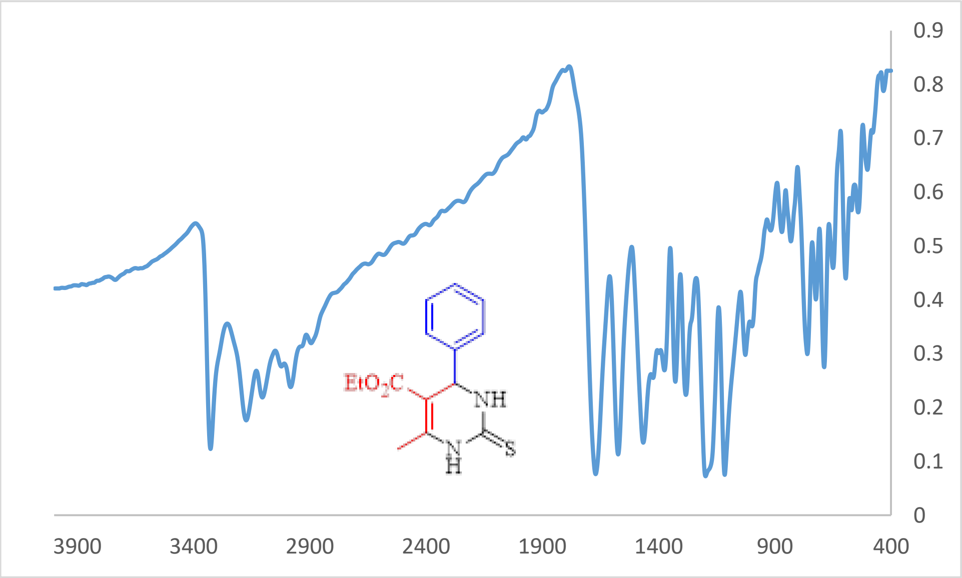

Fig. S17. FTIR spectrum of Ethyl 6-methyl-4-phenyl-2-thioxo-1,2,3,4-tetrahydropyrimidine-5-carboxylate (**4u**).

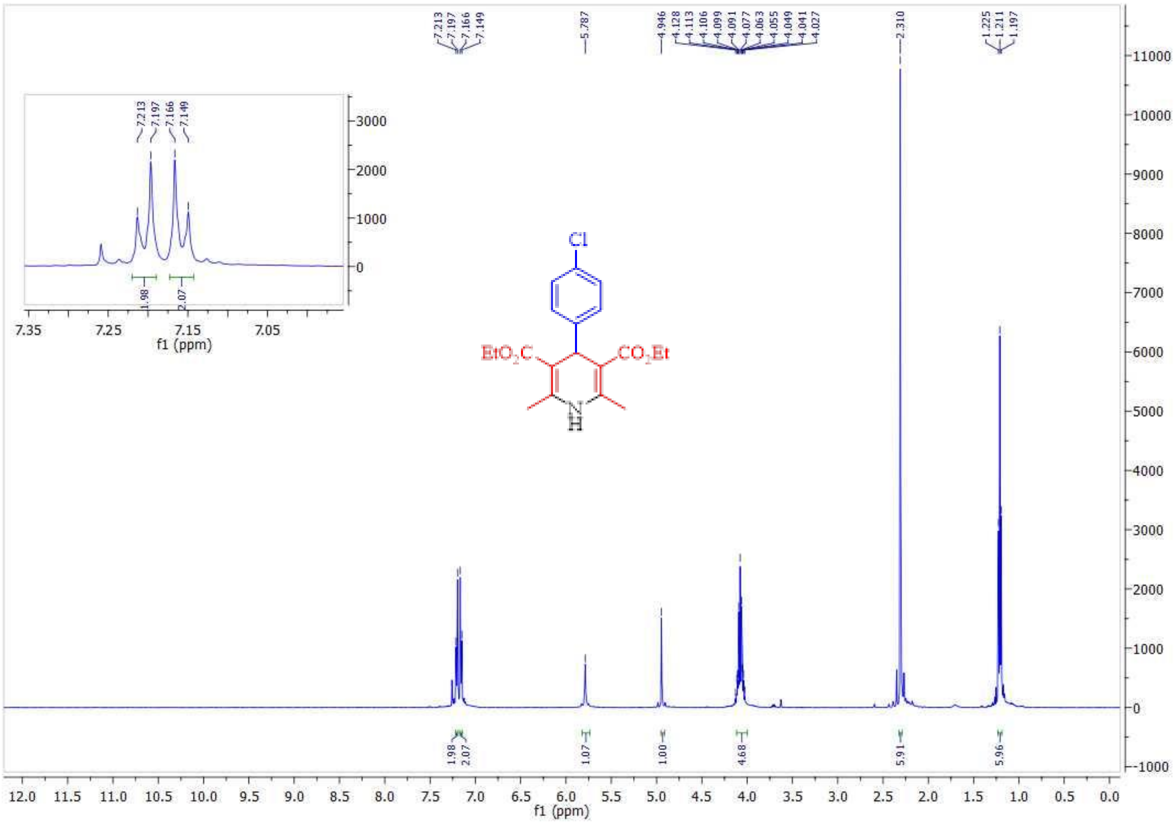

Fig. S18. ^{1}HNMR (500 MHz, DMSO-d$_6$) spectrum of Diethy l2,6-dimethyl-4-(4-colorophenyl)-1,4-dihydropyridine-3,5-dicarboxylate (**6c**).

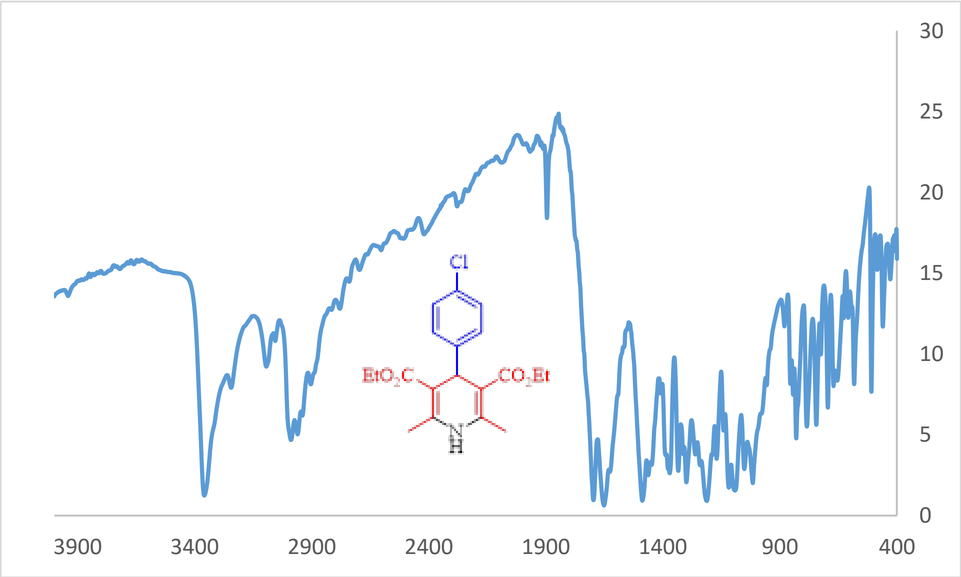

Fig. S19. FTIR spectrum of Diethy l2,6-dimethyl-4-(4-colorophenyl)-1,4-dihydropyridine-3,5-dicarboxylate (**6c**).

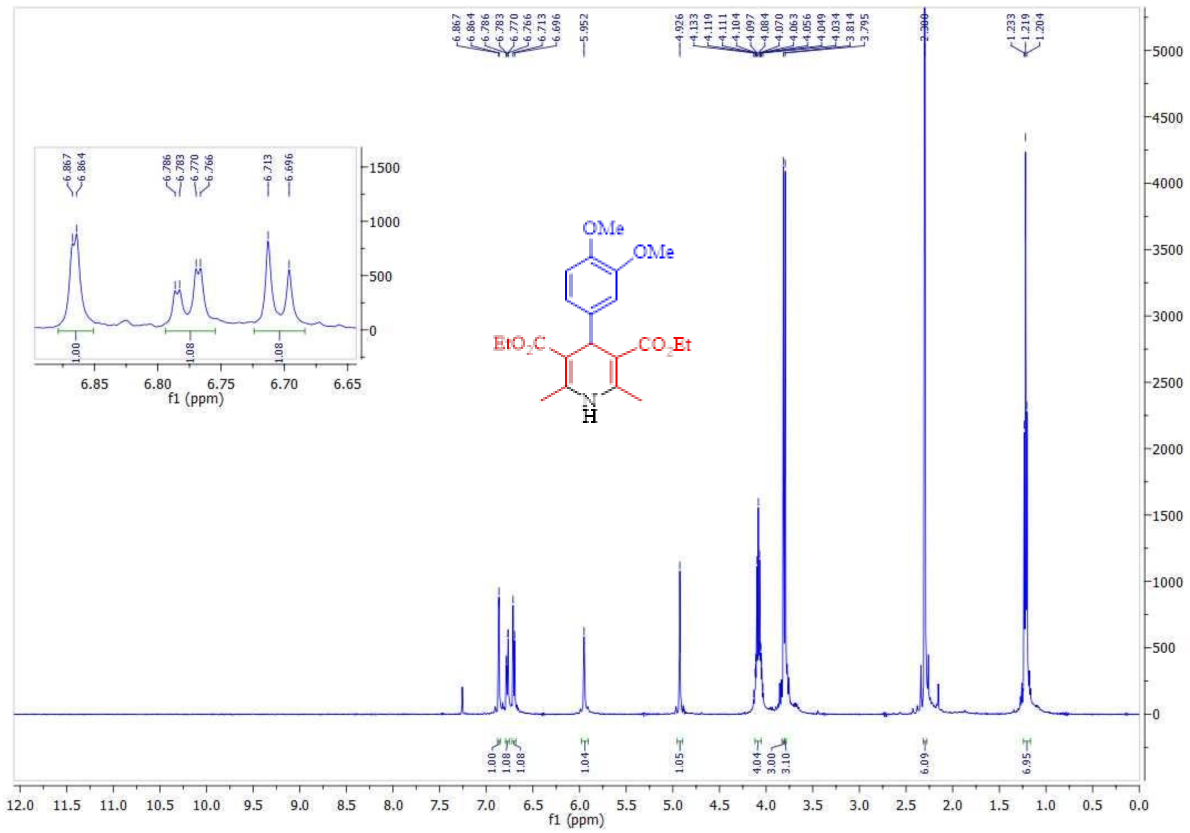

Fig. S20. ^{1}HNMR (500 MHz, DMSO-d$_6$) spectrum of Diethyl 4-(3,4-dimethoxyphenyl)-2,6-dimethyl-1,4-dihydropyridine3,5-dicarboxylate (**6h**).

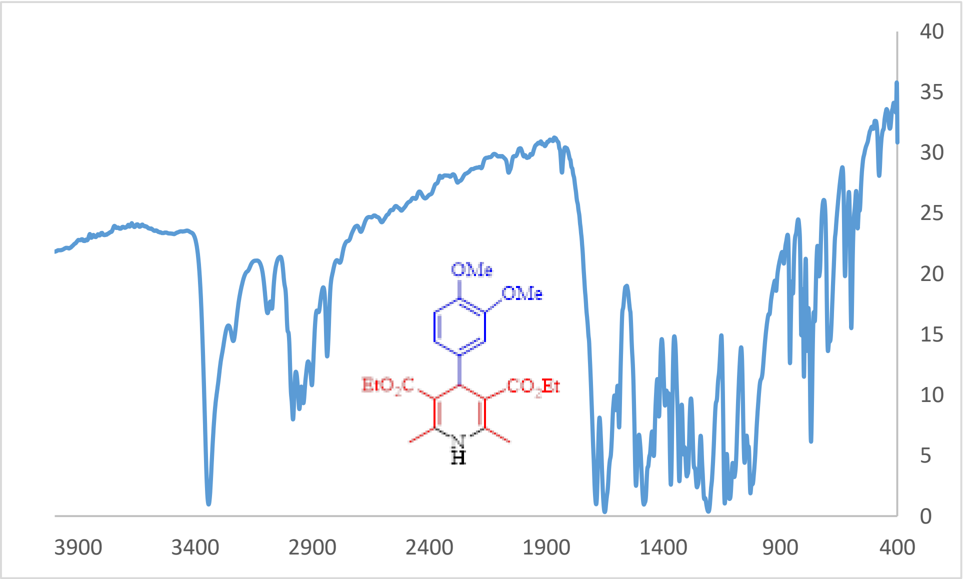

Fig. S21. FTIR spectrum of Diethyl 4-(3,4-dimethoxyphenyl)-2,6-dimethyl-1,4-dihydropyridine3,5-dicarboxylate (**6h**).

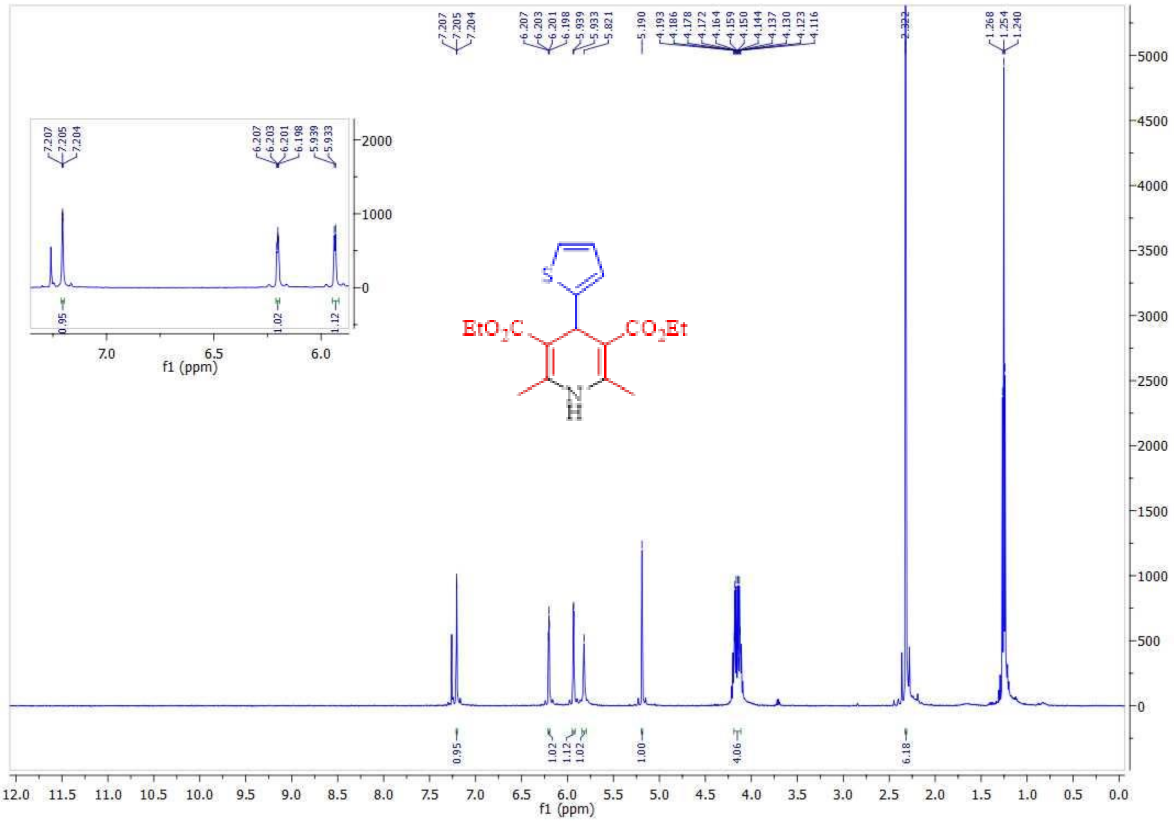

Fig. S22. ^{1}HNMR (500 MHz, DMSO-d$_6$) spectrum of Diethyl2,6-dimethyl-4-(thiophen-2-yl)-1,4-dihydropyridine-3,5-dicarboxylate (**6l**).

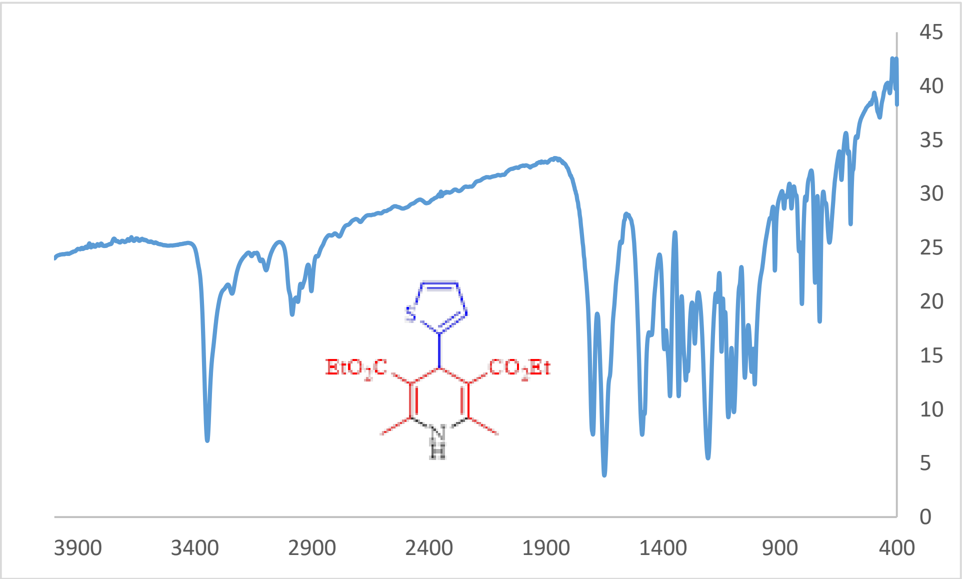

Fig. S23. FTIR spectrum of Diethyl2,6-dimethyl-4-(thiophen-2-yl)-1,4-dihydropyridine-3,5-dicarboxylate (**6l**).